CSIRO CLIMATE ADAPTATION FLAGSHIP
www.csiro.au

# BUSHFIRE DECISION SUPPORT TOOLBOX RADIANT HEAT FLUX MODELLING

## Case Study Two: Wangary, South Australia

Glenn Newnham[1,3], Raphaele Blanchi[2,3], Anders Siggins[1,3], Kimberley Opie[1,3], Justin Leonard[2,3]

1. CSIRO Land and Water

2. CSIRO Ecosystem Sciences

2. CSIRO Climate Adaptation Flagship

December 17, 2013

Report to the Bushfire Cooperative Research Centre

bushfire CRC

## Citation

Glenn Newnham, Raphaele Blanchi, Anders Siggins, Kimberley Opie, Justin Leonard (2013). Bushfire Decision Support Toolbox Radiant Heat Flux Modelling: Case Study Two, Wangary, South Australia, CSIRO report to the Bushfire CRC.

## Copyright and disclaimer



## Important disclaimer



## Acknowledgements

The authors would like to acknowledge the Bushfire Corporative Research Centre for ongoing support of this research. This report benefitted from insightful reviews by Dr Jacqueline England and Mr Tim Schenkels. We would like to thank one anonymous reviewer for his detailed comments regarding the Wangary Fire, particularly pertaining to the treatment of fuel load in the modelling of radiant heat flux.

# Executive summary


This report is a component of a broader research program being conducted within the Bushfire Cooperative Research Centre for the development of a house and community level Bushfire Decision Support Tools. One aim of the project is to extend the understanding of hazard classification under the current Australian Standard for Construction of Building in Bushfire Prone Areas (AS3959). This report details the second of three case studies used to develop spatial modelling of radiant heat flux incident on a house during a fire and to assess the significance of this modelled radiant heat on historic house loss.

The case study uses data collected during and after the fire that occurred at Wangary in South Australia in January 2005. The study develops detailed modelling of radiant heat incident on houses using detailed topographic information, while accounting for all types of vegetation present across the landscape. Case Study One (Siggins et al., 2013) used spatially detailed fuels information based on airborne lidar data. This case study extends Case Study One by investigating the feasibility of applying landscape level radiant heat modelling where only coarse fuels information is available.

A key finding of this research is that radiant heat flux modelled using coarse fuels information was a significant indicator of house damage in the case of the Wangary fire. Specifically, the total accumulated energy and the duration of exposure to radiant heat flux greater than 12 kW/m$^2$ were significant predictor variables for house damage, where the house was located on a vegetated site (grassland/cropland or forest). This is despite the relatively low levels of radiant heat generated by the grass fuel dominated Wangary fire. While radiant heat is unlikely to have been the primary mechanism for house ignition it has been shown as a strong surrogate for hazard (independent of the attack mechanism) and may be correlated with the likelihood of embers based ignition and flame contact.

Although radiant heat was shown to be significant as an indicator of damage to houses on vegetated sites, there was no relationship shown for damage to homes located directly on unvegetated sites, even when vegetation was in relatively close proximity. We hypothesise that houses located in these urban and bare soil areas (as they have been classified in broad scale land cover datasets) may be subject to combustion of other non-vegetation fuels that are not accounted for within this broad scale fuel mapping framework.

Executive summary iii

1 Introduction 1

2 The Wangary Fire 2

3 Model Input Data 3

3.1 Fire Arrival Time and Direction ....3

3.2 Fuel Load and Vegetation Height ....4

3.3 Topographic Elevation and Slope ....4

3.4 House Locations and Building Materials ....5

4 Methods 6

4.1 Flame Intensity and Height ....6

4.2 Calculation of View Factor ....7

4.3 Attenuation by vegetation and topography ....8

4.4 Radiant Heat Flux ....8

5 Results 10

5.1 Houses Surveyed ....10

5.2 Modelled Radiant Heat Flux ....10

5.3 Modelled RHF by Fuel Type ....13

5.4 RHF as a predictor of house damage ....14

6 Discussion 16

7 Conclusion 18

8 References 19

# 1 Introduction

The Australian Standard for construction of building in bushfire-prone areas (Standards Australia, 2009) outlines methods to specify the level of hazard to which a property is exposed. This level of hazard is summarised as a Bushfire Attack Level (BAL) and depends on the dominant vegetation type, the setback from vegetation to the house, and the terrain slope of the site. Although the BAL is a categorical scale of six levels, each level is based principally on a threshold of radiant heat flux (RHF) expressed in physical units of radiant heat flux in $W/m^2$.

The Bushfire Decision Support Tools Project seeks to further understanding of the risk to homes through modelling of RHF in greater detail than is currently possible using the Australian Standard AS3959.

As one component of the Bushfire Decision Support Tools Project, this case study is the second of three case studies, and considers the fire event at Wangary in January 2005. Specifically this case study detailed methods for modelling radiant heat flux incident on a house and includes:

- detailed modelling of the effect of landscape-level topography on fire rate of spread;
- accounting for all vegetation types present in the landscape, not just the dominant vegetation type;
- estimating attenuation of RHF by vegetation and the ground surface along the line-of-sight between a house and the flame front.

The project also aims to assess the significance of RHF on house loss using historical fire and house loss data. This report outlines the second of three case studies for the Wangary fire in January 2005, where RHF modelling is applied and its significance in house loss quantified. Unlike case study one (Siggins et al., 2013) there were limited spatial data available for the Wangary fire, specifically the absence of any airborne lidar coverage for detailed assessment of fuel load, type and extent. For this reason, it was not practical to use the full three dimensional ray-tracing approach outlined in Case Study One.

For the Wangary fire, the RHF modelling used the two dimensional approach outlined in Siggins et al. (2013), which applies the turbid medium approximation of vegetation structure based on a simplified input fuel information. The two dimensional RHF modelling was extended in this study to incorporate specific rate of spread and flame length equations for both grassland and forested areas within the vicinity of the house. The assessment of impact on the house was also extended to incorporate metrics that described the accumulated energy on the house outer surface and the duration of house exposure above a threshold for unpiloted ignition of timber. These are important to assess if the fire exceeded the theoretical threshold of building failure.

# 2 The Wangary Fire

On Monday, 10 January 2005, a fire began in farmland north of the town of Wangary on the Eyre Peninsula, South Australia. The fire was initially contained but on Tuesday 11 January 2005, weather conditions deteriorated with the Grassland Fire Danger Index exceeding 160 (Tippins et al., 2005). The fire broke containment lines, spreading south east towards the township of North Shields. Later that same day, a change in wind direction forced the fire north-east along the coast through the townships of Green Patch, Poonindie, Whites Flat, Louth Bay, Whites River and Koppio. More than 77,000 hectares were burnt in the fire, mainly consisting of farm and scrubland that supported rapid fire spread (Blanchi and Leonard 2006). Nine people died and a total of 93 homes were burnt in the fire (Smith, 2005).

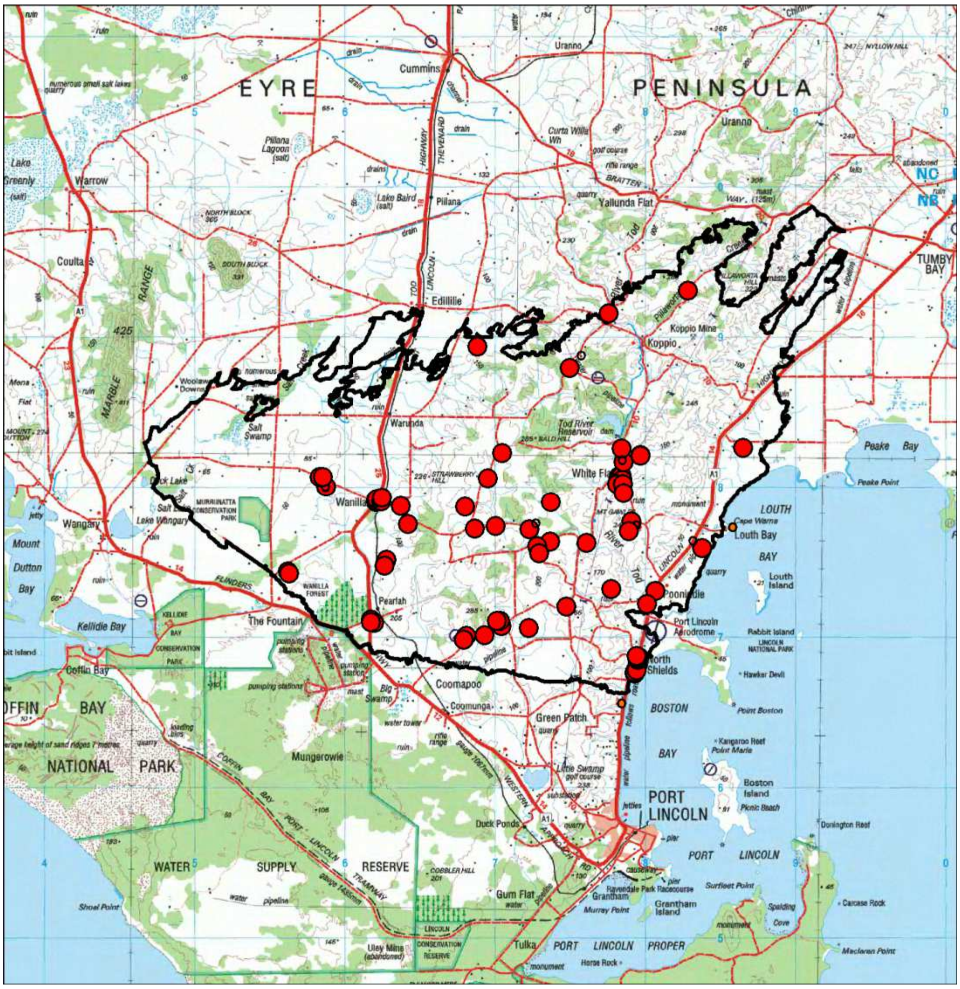


Figure 1: Spatial extent of the Wangary fire (——) and the distribution of burnt homes (●).

# 3 Model Input Data

## 3.1 Fire Arrival Time and Direction

The progression of the Wangary fire was described in detail by Gould (2005) and fire arrival times mapped using a series of isochrones. Spline interpolation was used to produce a continuous fire arrival time surface from these isochrones at a spatial resolution of 25 m on the same grid used by the National Carbon Accounting System (NCAS) remotely-sensed forest extent data (Furby, 2002). This surface, shown in grey scale in Figure 2, indicates the time in hours (*t*) on 11 January when the fire arrived at any location within the fire extent, including the arrival time at each structure.

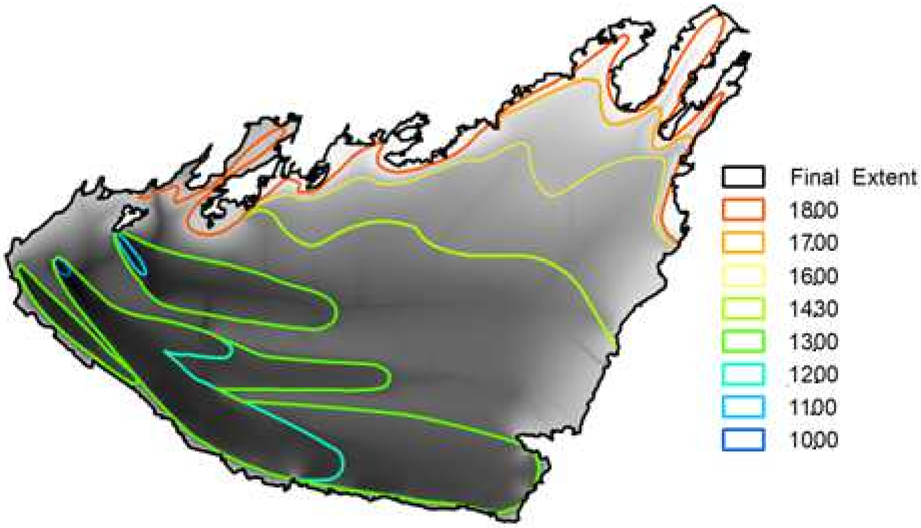


**Figure 2: The progression of the Wangary fire as defined by isochrones produced by Gould** (2005) **overlayed on the interpolated fire arrival time surface. The legend expresses 24 hour time on the day of 11 January 2005.**

Fire spread direction can be used to assess the specific fuels and topography that influenced the fire as it impacted a specific home or out-building. The derivation of a continuous fire direction surface can be achieved using methods similar to topographic aspect determination (e.g. Burrough and McDonnell, 1998). In this case, fire direction $\varphi$ is determined from the fire arrival time surface $t_{x,y}$ using the equation:

$$\tan(\varphi) = \frac{(t_{x-1,y-1} + 2t_{x,y-1} + t_{x+1,y-1}) - (t_{x-1,y+1} + 2t_{x,y+1} + t_{x+1,y+1})}{(t_{x+1,y-1} + 2t_{x+1,y} + t_{x+1,y+1}) - (t_{x-1,y-1} + 2t_{x-1,y} + t_{x-1,y+1})}$$

where subscript *x* refers to the pixel easting coordinate and subscript *y* refers to pixel northing and $\varphi$ is expressed in radians.

## 3.2 Fuel Load and Vegetation Height

Fuel loads are a critical input to fire rate of spread and intensity calculations. In the absence of high spatial resolution vegetation information (e.g. airborne lidar used in Case Study One), fuel loads were assigned based on land use classification data, in similar categories to those used in AS3959 (Standards Australia, 2009).

The Australian Land Use and Management (ALUM) classification was developed for the Murray-Darling Basin Commission (Baxter and Russell, 1994). Version 6 of the ALUM national classification dataset (ABARES, 2010) provides spatially and thematically detailed land cover information at 25 m spatial resolution as at 2008, three years after the Wangary fire. The National Carbon Accounting System (NCAS) forest/non forest product (Furby, 2002) provides yearly forest extent information, again at 25m resolution. NCAS data for the Eyre Peninsula were available for 2004, one year prior to the Wangary fire. These two datasets were combined to provide a detailed land cover classification, with NCAS taking priority for defining forest spatial extent and ALUM providing detail on vegetation type in non-forested areas. Overall fuel loads were assigned as prescribed by AS3959 as shown in Table 1. Height for all vegetation classes is used for determining attenuation of RHF between a home and the flame front. Estimated mean vegetation heights for each vegetation class are shown in Table 1.

**Table 1: Vegetation types derived from the ALUM and NCAS datasets and their assigned overall fuel loads and estimates mean heights**

| Fuel Type | Surface Fuel Load (t/ha) | Overall Fuel Load (t/ha) | Vegetation Height (m) |
|---|---|---|---|
| Forest | 25 | 35 | 20 |
| Woodland | 15 | 25 | 10 |
| Shrubland | 15 | 15 | 1.5 |
| Pasture | 4.5 | 4.5 | 0.1 |
| Cropping | 4.5 | 4.5 | 0.5 |
| Grassland | 4.5 | 4.5 | 0.5 |
| Non-vegetated | 0 | 0 | 0 |

Final overall fuel load and vegetation height information was resampled on the NCAS 25 m spatial resolution grid to align with fire arrival time and direction data.

## 3.3 Topographic Elevation and Slope

Topographic information, in the form of a digital elevation model, is required to derive the slope for input to rate of spread calculations, as well as to determine any shadowing of the flame at a house location by the ground surface. In Case Study One (Siggins et al., 2013), terrain attributes and slope were derived at high spatial resolution from airborne lidar data. As these data were not available for the Eyre Peninsula, we used a Shuttle Radar Topographic Mission (SRTM) derived smoothed digital elevation model at 30 metre pixel resolution (Gallant et al., 2011). This DEM-S product, as it is referred to by Gallant et al. (2011), removes many of the errors in raw SRTM data caused by sensor artefacts and limited penetration through forest canopies. The SRTM based DEM was resampled to align with the NCAS 25m spatial resolution grid.

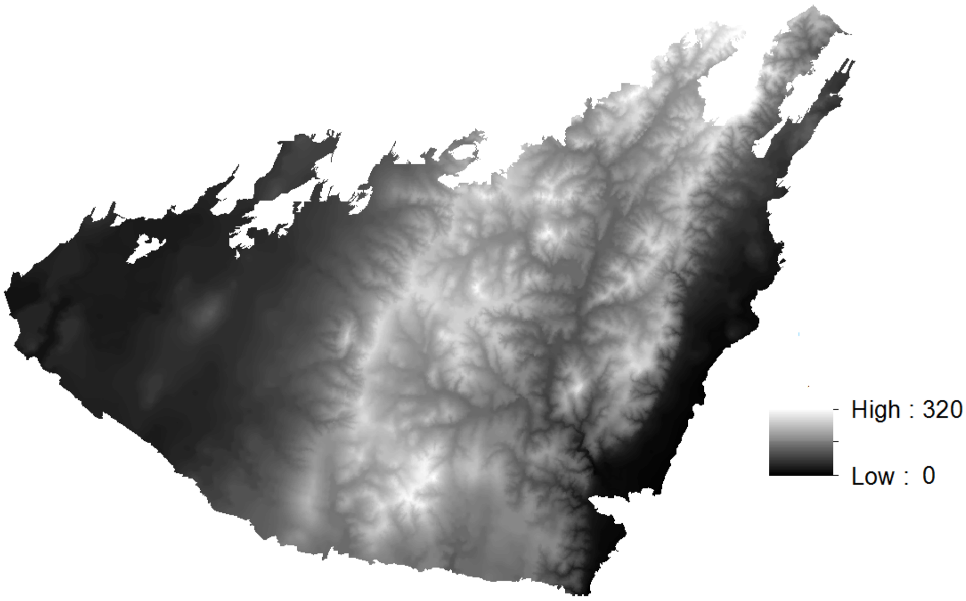


**Figure 3: Digital elevation model for the Wangary fire extent based on Shuttle Radar Topographic Mission data. Elevations range from sea level to a maximum of 320 m.**

## 3.4 House Locations and Building Materials

A detailed house survey was carried out after the Wangary fire from 17 to 21 January 2005 by teams from the Bushfire CRC, Geoscience Australia, the South Australian Country Fire Authority, South Australia Police and CSIRO. The survey focussed on houses impacted by the fire and recoded the level of damage along with details of building construction and materials. Damage status was recorded for 80 homes, most of which were destroyed by the fire. However, some less heavily impacted homes within the final fire extent were also surveyed (Figure 4).

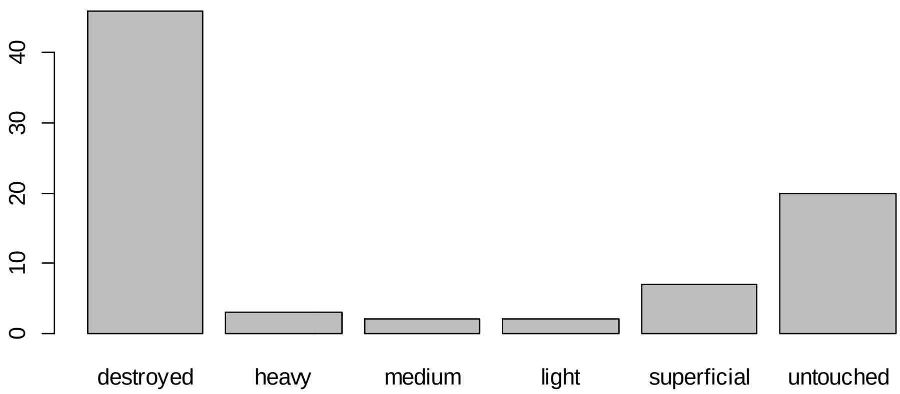


**Figure 4: Number of homes surveyed after the Wangary fire in each of five damage level classes. A description of the survey methods and classes is contained in** Leonard and Blanchi (2006)

# 4 Methods

## 4.1 Flame Intensity and Height

The two-dimensional RHF model outlined by Siggins et al. (2013) uses the empirical equations employed by AS3959 (McArthur, 1973a, 1973b; Noble et al., 1980) to determine fire and flame characteristics. The primary difference in the two-dimensional approaches is that the input to the McArthur equations are derived using spatially explicit data along a 100 metre transect in the fire approach direction from each affected home. Each transect is sampled at 1m intervals to determine the appropriate fuel and terrain attributes for input to fire spread and intensity modelling.

In Siggins et al. (2013) only forest fire spread and intensity equations were used. Given the additional thematic detail provided by the ALUM data, it was possible to use the fire rate of spread equations (McArthur, 1973a, 1973b; Noble et al., 1980) for both forest and grassland:

| | |
|---|---|
| Forest | $R = 0.0012 \times FFDI \times w$ |
| Grassland | $R = 0.13 \times GFDI$ |

where $FFDI$ is the MacArthur Forest Fire Danger Index (McArthur, 1973a), $w$ is the surface fuel load and $GFDI$ is the MacArthur Grassland Fire Danger Index (McArthur, 1973b). We have used the $FFDI$ of 100 reported by Tippins et al. (2005) for 1 pm on the day of the fire, along with the $GFDI$ equivalent of 130 (Standards Australia, 2009).

Slope correction was employed to all rate of spread values based on 10m weighted moving average filtering of the DEM-S data along each 100m transect. The correction for slope expressed in degrees ($\theta$) is specified by Noble et al. (1980) as:

$$R_{slope} = R \times e^{0.069 \times \theta}$$

where $\theta$ is positive for an upward slope approaching the house and negative for a downward slope. In either case the slope is limited to a maximum of 15 degrees as per AS3959. Based on this corrected rate of spread and the overall fuel load ($W$) in t/ha (see Table 1), we calculate the fire intensity ($I$) in $kW/m^2$ using the AS3959 approach (Byram, 1959) as follows:

$$I = \frac{H \times W \times R_{slope}}{36}$$

where $H$ is the heat of combustion ( ~ $18600 KJ.Kg^{-1}$). Flame length ($L_f$) is a critical parameter for the two dimensional RHF model as the RHF associated with the portion of the flame below the vegetation height is attenuated by vegetation along the line of sight to the house. The portion of the flame that protrudes from the top of the canopy may provide a clear path for radiant heat to receiver location. The estimation of $L_f$ is based on Noble et al. (1980) for forest vegetation, while $L_f$ for grassland is based on the equation of Nelson (1980) as follows:

Forest $L_f = \left( (13 \times R_{slope}) + (0.24 \times W) \right) - 2$

Grassland $L_f = 1.192 \sqrt{\frac{I}{1000}}$

The forest flame length equation as specified by Nobel (1980) is thought to overestimate flame length. For this reason, a slightly modified equation is employed in AS3959 (Standards Australia, 2009). However, this equation is not detailed in the scientific literature, so we have adopted the citable equation for our modelling. .

The view of a flame from the perspective of a home is modified by flame angle. However, in practice it is difficult to determine an appropriate flame angle for RHF calculation. The AS3959 takes a worst case scenario approach, estimating the flame angle that will produce the highest RHF through iterative estimation. The following section describes an alternative approach to specifying flame angle that maintains this assumption of a worst case flame angle.

## 4.2 Calculation of View Factor

From the perspective of a point on a house or other asset that may be exposed to radiant heat, the proportion of the hemisphere in the direction of the fire front that flame can be observed is known as the view factor (Drysdale, 1985; Sullivan, 2003; Zárate et al., 2008). Resolving the view factor has been a key challenge to those attempting to predict radiation exposure levels on houses.

AS3959 specifies a fire front width of 100m, unless the width of classified vegetation justifies the use of a lesser value (Standards Australia, 2009). The azimuthal angular span for this 100m flame front ($\Delta\varphi_f$) is dependent on the horizontal range from a house ($r$) and the height difference between the receiver and the flame base $h(r)$. This angular span is given by:

$$\Delta\varphi_f = 2\,tan^{-1}\left(\frac{50}{\sqrt{r^2 + h(r)^2}}\right)$$

where $h(r)$ is the height of the terrain at distance $r$ in the direction from which the fire is approaching relative to the view point on the house. The total view factor can then be calculated based on the proportion of the hemispherical view ($2\pi$ steradian) from which radiant heat is emanating:

$$\emptyset = \frac{\int_0^{\Delta\varphi_f} \int_{\theta}^{\theta+\Delta\theta} sin\theta d\theta d\varphi}{2\pi}$$

$$\theta = \frac{\pi}{2} + tan^{-1}\frac{h(r)}{r}$$

$$\Delta\theta = 2\,sin^{-1}\frac{L_f}{2\sqrt{r^2 + h(r)^2}}$$

where $\theta$ is the zenith angle to the base of the fame and $\Delta\theta$ is the angular height of the flame with flame front normal to the viewing vector such that the assumption of the worst case flame angle is incorporated. This integral can be approximated as a trapezium:

$$\emptyset(r) = \frac{\Delta\varphi_f[cos\,\theta - cos(\theta + \Delta\theta)]}{2\pi}$$

## 4.3 Attenuation by vegetation and topography

The view factor described in the previous section assumes no attenuation of radiant heat by vegetation or the ground surface (topographic shading). Attenuation can be incorporated into the existing AS3959 framework for modelling RHF through a reduction in the view factor. Attenuation is assessed by sampling regular intervals along the line of sight between $\theta$ and $\Delta\theta$ to determine if ground or vegetation is encountered. If neither is present then the attenuation is set to zero. If ground is encountered then the attenuation at this location in space is set to one. If vegetation is encountered then attenuation depends on the projected area of the foliage, or plant area density (Takeda et al., 2008). Plant area density was shown by Jupp et al. (2009) to peak at around 0.15 for an Australian Eucalyptus forest canopy. In cases where vegetation is encountered along the line of sight, attenuation $\alpha$ over the horizontal increment in range $\Delta r$ is given by:

$$\alpha = cos\,\theta\,(1 - e^{-PAD})\Delta r$$

where *PAD* is plant area density. The view factor along a line of sight at angle $\theta$ between a house and a flame front at horizontal range $r$ is simply product of the complement of all attenuation coefficients encountered:

$$\emptyset(r,\theta) = \prod_{x=0}^{x=r} 1 - \propto_x$$

Thus accounting for attenuation, the view factor for the flame at range r becomes:

$$\emptyset(r) = \frac{\int_{\theta}^{\theta+\Delta\theta}[\prod_{x=0}^{x=r} 1 - \propto_x]\,d\theta}{4\pi} \times \Delta\varphi_f$$

## 4.4 Radiant Heat Flux

If the flame front is considered as a uniform diffuse black-body emitter (Sullivan et al., 2003), as is currently the case for the Australian Standard AS3959, then the level of radiant heat flux incident on a house from a flame front at horizontal range $r$ depends on the Stefan–Boltzmann law:

$$RHF(r) = \emptyset(r)\,\varepsilon\,\sigma\,T^4$$

In units of $kW.m^{-2}$, where $\varepsilon$ is the emissivity for vegetation (assumed to be 0.95), $\sigma$ is the Stefan Bolztman constant ($5.67x10^{-11}$ $kW.m^{-2}.K^{-4}$), $T$ is the flame temperature (assumed to be 1200K as used in Siggins et al. 2013; the temperature isbased on the most conservative temperature specified by AS3959 (CFA, 2013) and discussed in Leonard, 2013.

The result of the two-dimensional modelling is a range (and therefore time) dependent RHF profile. These profiles were generated for each house surveyed after the Wangary fire along 100 metre transects in the direction of the fire approach direction. A number of summary statistics based on these $RHF$ profiles are assessed in the results section. This includes the total RHF for each 100m transect, maximum $RHF$ values and the range at which threshold maximum RHF levels was achieved. Given the observations of Tran et al. (1992) we also determined the range at which the minimum threshold for ignition of timber building material was achieved (12 $kW/m^2$). Total energy accumulation is also calculated from each RHF profile based on the equation:

$$E = \int_{r=0}^{100} \frac{RHF(r)}{R_{slope}(r)}\, dr$$

where E is in $kJ.m^{-2}$. The significance of these RHF statistics were determined using the separability of their distributions for damaged and undamaged homes. Logistic regression modelling was used as a measure of the capability of each metric for predicting house damage based on modelled $RHF$ exposure.

# 5 Results

## 5.1 Houses Surveyed

Isochrones derived surfaces indicated that most of the homes surveyed were impacted by the Wangary fire between 1pm and 2pm on 11 January 2005. Homes were generally located in areas of agricultural or open grassland, according to ALUM and NCAS data, leading to low modelled fuel loads and low vegetation heights. Of the 80 homes, 40 were located within grassland or cropland, five within the forest and 35 on unvegetated ground (predominantly urban and bare ground in ALUM). The homes 5 located within the forest extent were classified as damaged, 31 of the 40 homes located in grassland were damaged, while 15 of 35 houses located in unvegetated ground were damaged.

Due to the limited sample size of the house survey (80 homes), damage categories shown in Figure 4 were collapsed into two classes for the purpose of analysing RHF characteristics. Destroyed, heavy and medium homes were considered ‘damaged’ (51 homes), while light, superficial and untouched homes were considered ‘undamaged’ (29 homes).

## 5.2 Modelled Radiant Heat Flux

The characteristics of the RHF incident on houses located in grassland were predictably quite different to those located within a forest. Fire intensity and flame height in the immediate vicinity of the house should be expected to be greater for forested sites. However, a greater proportion of the radiant heat emanating from a distant flame front should also be expected to be attenuated by nearby vegetation. Two example RHF profiles are shown in Figure 5 and Figure 6, along with respective fuel load, terrain and fire intensity.

Figure 5 shows the RHF profile for a house located in non-vegetated (cleared) land. The edge of grassland is at a range of 33m and the forest edge is at a range of 69m in the direction from which the fire approached along a gently sloping (< 1 degree) terrain. As the fire approaches through the forest, fireline intensity peaks at 83.1 kW/m at a range of 93 m, but RHF is attenuated by the vegetation between the flame front and the house. Peak RHF is experienced when the flame reaches the near edge of the forest at 69 m at 10.3 kW/m$^2$. RHF then drops as the fire enters grassland, but increases to 5.1kW/m$^2$ as it reaches the near edge of grassland where there is no longer any attenuation of the RHF and the view factor has increased due to the proximity of the flame. Once the fire reaches the non-vegetated area at 32 m from the house, the lack of fuel means that the intensity and RHF drops to zero.

Figure 6 shows the profile for a house located in grassland with the forest edge at 23 m. The terrain in the fire approach direction slopes steeply downward reaching in excess of 15 degrees. As the fire approaches through the forest, fire intensity is amplified in steep upward sloping areas, although a 15 degree limit is applied for rate of spread calculations. The 15 degree slope limit can be seen in the fireline intensity calculation, which imposes a hard limit of 213.8 kW/m at a range of 39 m. At the forest edge (23m from the house) the RHF reaches 36.1 kW/m$^2$, but continues to climb as the fire progresses through grassland towards the house. The RHF reaches a maximum of 108.8 kW/m$^2$ as the flame reaches the house.

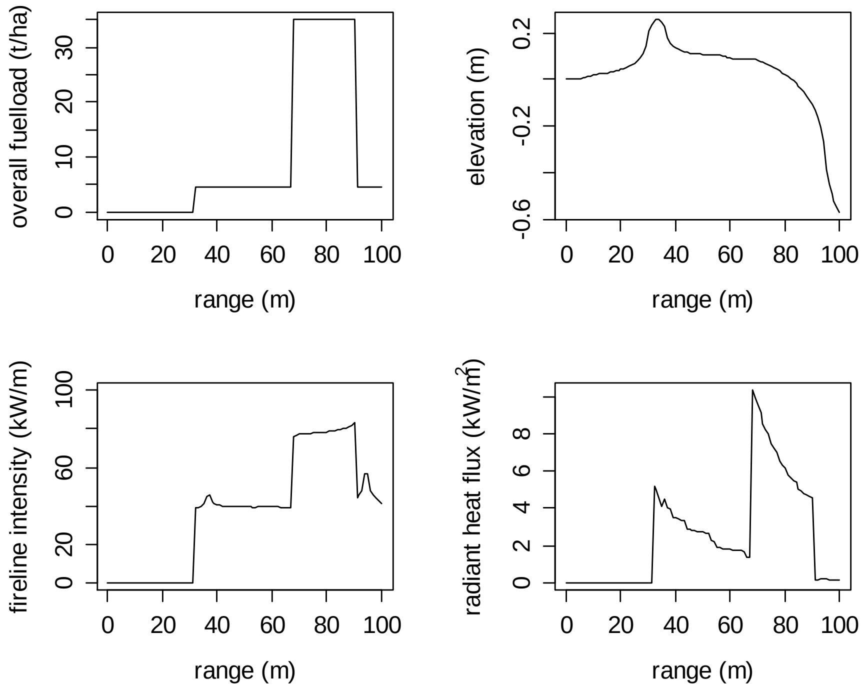


**Figure 5: Transects sampled from a home on a non-vegetated site out to 100m in the fire approach direction. Forest is encountered at 60m which leads to high fire intensities, which are significantly moderated by a gradual downward slope towards the house.**

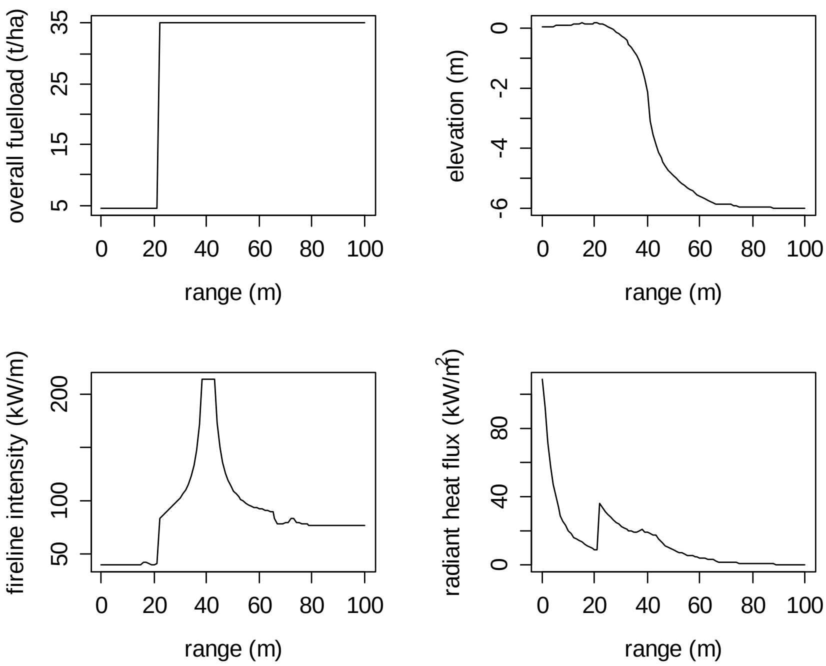


**Figure 6: Transects sampled from a home on a grassland site out to 100m in the fire approach direction. Forest is encountered at 20m which leads to high fire intensities, which are exacerbated by a steep upward slope towards the house.**

Mean RHF profiles for damaged and undamaged homes in the survey are shown in Figure 7. There is very little separation in the profiles at ranges greater than 40m. Nearer to the homes the mean profile for the sub-set of damaged homes is higher and the mean difference increases as the fire approaches. A paired t-test showed a significant difference of the mean profiles ($t = 4.12$, df = 100 range samples, p-value $< 0.001$).

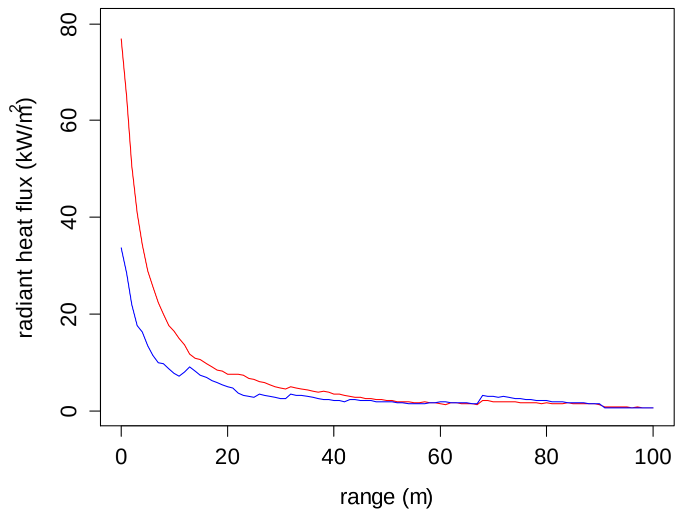


**Figure 7: Mean modelled radiant heat flux (RHF) profiles for all damaged (red) and undamaged (blue) homes surveyed after the Wangary fire.**

Modelled RHF profiles for the 80 homes surveyed were summarised using simple metrics to determine their significance in predicting damage (and ultimately predicting risk). Summary statistics included:

- The maximum *RHF* value along the 100m transects in $kW/m^2$;
- The range from the house at which the maximum *RHF* occurred in metres;
- The total accumulated energy at the house surface in $kJ/m^2$;
- The total time of exposure to RHF greater than $12kW/m^2$ in seconds.

As shown in Table 2, damaged homes on average were subject to 34.5 $kW/m^2$ higher maximum RHF. The range from the house at which this maximum occurred on average 10.7 m less for damaged homes. We found the greatest separability between damaged and undamaged homes (using Welch Two Sample t-test) was through the maximum RHF (Table 2). The range from the house at which the maximum RHF occurred was not significantly different between damaged and undamaged homes. However for damaged homes the accumulated energy at the house surface was separable at the 97.5% confidence level: similarly the time of exposure to greater than $12kW/m^2$ was separable at the 95% confidence level.

**Table 2: Summary of RHF profile statistics for damaged and undamaged homes surveyed after the Wangary fire**

| Variable | Mean Damaged | Mean Undamaged | p-value |
|---|---|---|---|
| *Maximum RHF* ($kW/m^2$) | 78.8 | 44.3 | 0.002 |
| *Range to Max RHF (m)* | 13.3 | 24.1 | 0.130 |
| *Accumulated Energy* ($kJ/m^2$) | 19.1 | 12.3 | 0.025 |
| *Time* > $12\ kW/m^2$ *(s)* | 4.8 | 2.6 | 0.051 |

## 5.3 Modelled RHF by Fuel Type

Although maximum RHF provided statistical separability between damaged and undamaged classes, the distribution of maximum RHF was very different for houses located in the three major land cover types (Figure 8a). For houses located within grassland/cropland or forest, the maximum RHF was clustered around 108 kW/m$^2$. The lack of variability is due to the view factor for a flame at zero distance (Figure 8b) reaching near the maximum of one under both fuel loads.

The distribution of maximum RHF for homes located in unvegetated areas (urban and bare soil areas) was more variable and depended on the distance to fuel along the profile in the fire approach direction. However, generally high maximum RHF levels were associated with houses that were not damaged by the fire.

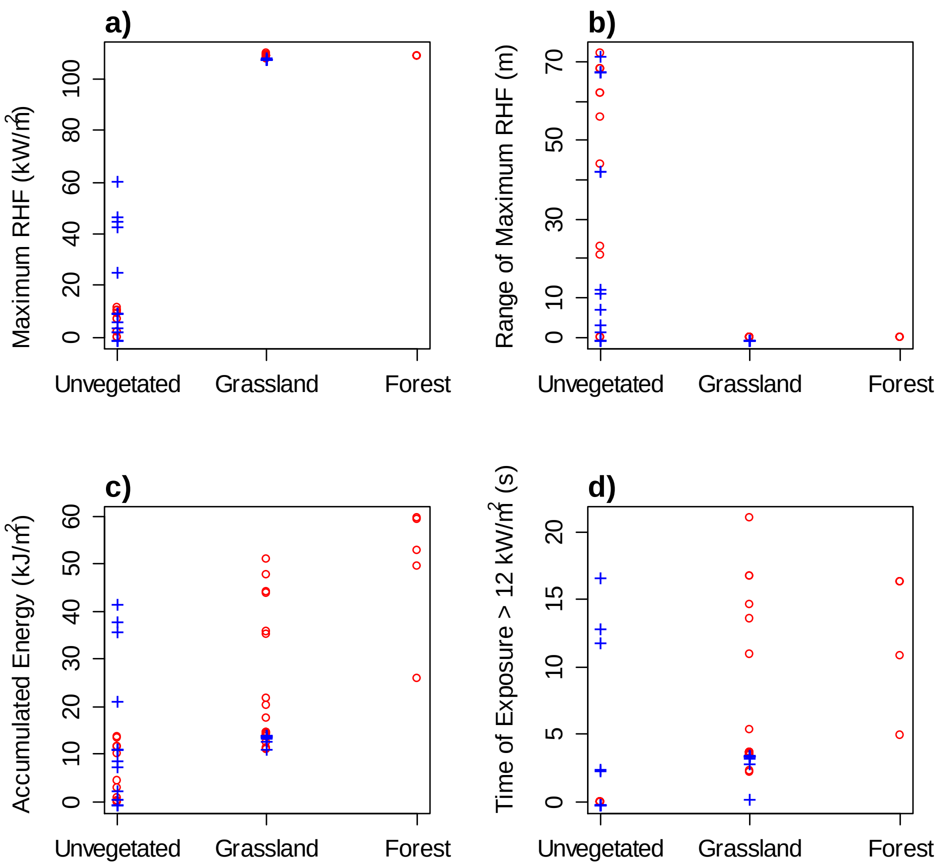


**Figure 8: Distribution of a) maximum RHF b) the range from the house at which this maximum RHF occurred, c) the total accumulated energy load at the house and d) the duration of exposure to greater than 12 kW/m$^2$ of radiant heat flux. Distributions are shown for homes located in each of the three major fuel types (unvegetated, grassland/cropland and forest) and separated into damaged (o) and undamaged (+) homes.**

The total accumulated energy (Figure 8c) and the duration of exposure to greater than 12kW/m$^2$ (Figure 8d) provided greater variance for grassland and forest classes. Damaged homes located in forest and grassland areas tended to have been exposed to greater levels of accumulated energy and were exposed to greater than 12kW/m$^2$ for longer durations. However, the unvegetated class did not show a similarly predictable higher exposure levels for damaged homes. In the unvegetated class, damaged homes tended to show higher accumulated energy levels and greater durations of exposure to greater than 12 kW/m$^2$.

## 5.4 RHF as a predictor of house damage

While the RHF profiles did not appear to have a strong relationship to house damage for houses in unvegetated areas, they did show potential as an explanatory variable for houses located within grassland/cropland and forest. Binary logistic regression models were fitted to damage status {damaged, undamaged} based on both accumulated energy and the duration of exposure to greater than 12 kW/m$^2$ of radiant heat flux. Both models were significant for explaining damage to houses (Table 3). The use of both variables in a multivariate logistic model resulted in an increase in the Akaike Information Criterion (AIC), indicating a relative drop in the goodness of fit of the model given the added complexity of using two parameters.

**Table 3: Summary of models for the probability of house damage based on the total accumulated energy and the duration of exposure to greater than 12 kW/m$^2$. The relative performance for the models was similar based on the Akaike Information Criterion (AIC). Both models were shown to be significant at the 99% confidence level based on the $\chi^2$ statistic.**

| Explanatory Variable | Mean Damaged | Mean Undamaged | AIC | p-value |
|---|---|---|---|---|
| *Accumulated Energy (kJ/m$^2$)* | 24.234 | 13.96 | 42.16 | >0.01 |
| *Time > 12 kW/m$^2$ (s)* | 6.828 | 3.165 | 41.96 | >0.01 |

Logistic models are based on the log of the ratio of the probability of damage verses the probability of no damage so the equation for each model is an exponential function of each explanatory variable as follows:

$$P_{dam}(E) = \frac{e^{-2.9+0.18E}}{1 + e^{-2.9+0.18E}}$$

$$P_{dam}(T_{>12}) = \frac{e^{-2.2+2.13T_{>12}}}{1 + e^{-2.2+2.13T_{>12}}}$$

where $P_{dam}$ is the probability of house damage, $E$ is the total accumulated energy at each house and $T_{>12}$ is the duration of the exposure of each house to greater than 12 kW/m$^2$. The form of these models is shown in Figure 9. These indicate that a probability of 90 percent damage is reached when the total accumulated energy reaches 19 kJ/m$^2$ or when the duration of exposure to 12 kW/m$^2$ is greater than five seconds. The probability of damage rises to 99 percent when the total accumulated energy reaches 28 kW/m$^2$ or when the duration of exposure to 12 kW/m$^2$ of 9 seconds.

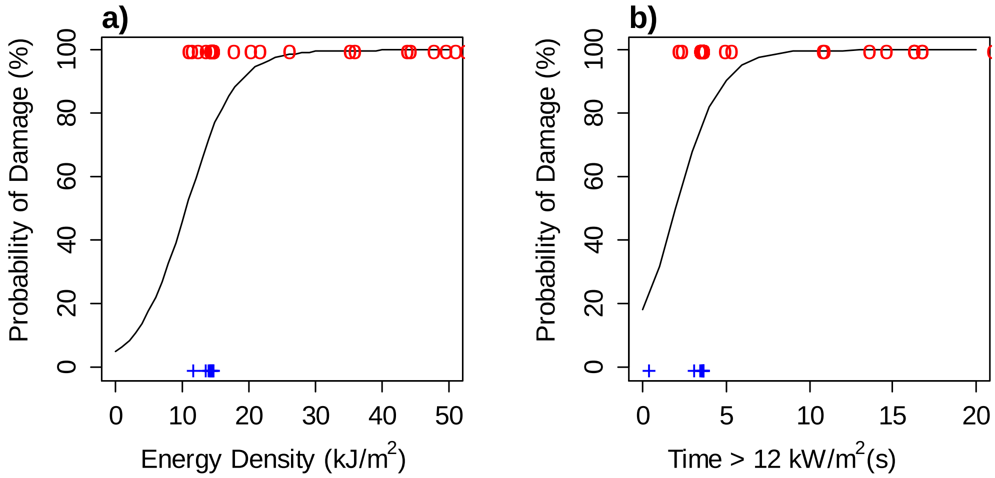


**Figure 9: Binary logistic regression models for the probability of damage to homes based on a) total accumulated energy and b) the duration of exposure to greater than 12 kW/m$^2$ of radiant heat flux. Damaged (o) and undamaged (+) homes are shown in their respective total accumulated energy and exposure duration locations. Only homes that were located in vegetated areas are included in the models.**

# 6 Discussion

In a previous study, Siggins et al. (2013) presented a full three dimensional ray tracing approach for modelling radiant heat flux incident on homes during a bushfire. This model used vegetation structure derived from airborne lidar data to build the three dimensional simulation environment in which modelling was performed. Airborne lidar provides very detailed vegetation structural information that is unparalleled for landscape level analyses and can be used to estimate fuel distribution and the effect of vegetation on radiant heat attenuation. Despite the growing frequency and spatial extent of airborne lidar data captured in Australia, airborne lidar is not always available at the precise location and time required for post-fire analysis or hazard prediction.

For the Wangary fire of 2005, suitable airborne lidar was not available for characterising the pre-fire vegetation structure. As a compromise, we employed existing lower spatial resolution (25m) federal government datasets for the purpose of determining fuel characteristics. Given that these datasets have national coverage, this represents a worst case scenario for vegetation information as an input to predictive radiant heat flux modelling.

Despite the limited input data, we have shown that it is possible to model radiant heat as a flame progresses towards individual houses, taking into consideration variations in fuel load, topography and attenuation caused by topographic shadowing and vegetation between the fire front and the house. The fire rate of spread, line intensity and radiant heat flux modelling are all based on existing empirical equations (McArthur, 1973b, 1973a; Noble et al., 1980) used in the Australian Standard AS3959 for construction of buildings in bushfire prone areas (Standards Australia, 2009). However, by considering broader site characteristics this study has allowed consideration of multiple fuel types and complex site topographies that is not possible under the AS3959 approach. The model presented also enables considerations of attenuation by fuels that fall between the fire front and the house, which has been cited as a factor in houses survival (Leonard, 2009; Cohen, 2004).

The accuracy of models used in AS3959 (McArthur, 1973b, 1973a) have been questioned, particularly as they relate to fire spread and flame characteristics under extreme weather conditions (Teague et al., 2009). A number of alternative models have been proposed that seek to address these limitations (e.g. Cheney et al., 1998), which could be incorporated into the radiant heat flux modelling approach presented in this work, given adequate information about the spatial distribution of input parameters.

Characteristics of the radiant heat flux profiles produced through RHF modelling have been shown to be significant as an indicator of house damage during the Wangary fire. Specifically, the total accumulated energy and the duration of exposure to RHF greater than 12 kW/m$^2$ were shown to be significant explanatory variables in binary logistic models of house damage where the house is located on a vegetated site (grassland/cropland or forest). This is despite the fact that radiant heat is unlikely to have been the primary mechanism for house ignition, based on the 30 second exposure at greater than 12 kW/m2 threshold cited by Tran et al. (1992). This may be due to the fact that the level of radiant heat exposure is a strong indicator of the prevalence of embers based ignition and flame contact.

The characteristics of RHF profiles were not significant explanatory variables for damage to houses located on unvegetated sites (urban, bare soil, etc). This is most likely because neither radiant heat nor high intensity ember based ignition occurred in these areas. Ignition in these areas are more likely to occur due to combustion of low level ground fuels and other combustible elements immediately adjacent to the building, neither of which were captured within the low resolution fuel information available for the study (Leonard et al., 2011). In addition, unvegetated sites are also likely to benefit from a higher prevalence of active defence. This may explain why some houses on unvegetated sites did not sustain damage while being exposed to high levels of RHF (see Figure 8).

In a number of cases, ember attack has been shown to be the most significant cause of house damage during Australian bushfires (Blanchi and Leonard, 2008), particularly where grassland and cropland are the dominant fuel source (Leonard and Blanchi, 2006). The model presented here lacks explicit consideration of ember exposure and flame contact for houses surveyed after the Wangary fire. Radiant heat flux modelling is used effectively as a surrogate for all exposure mechanisms with a moderate to high level of statistical correlation for houses surrounded by grassland and forest fuels. However there is a relatively poor correlation with houses that are located in unvegetated areas. This reliance on radiant heat exposure is a simplification of reality, and there is little doubt that additional improvements could be made by considering all bushfire attack mechanisms. This may include detailed landscape level analysis of ember load exposure, the probability of direct flame contact caused by the combustible elements that immediately surround homes.

# 7 Conclusion

The radiant heat flux modelling presented in this report is the second in a series of three case studies being used to develop methods for better site based assessments of bushfire hazard. These assessments of hazard can be used for informing decisions on site preparation and house construction which might ameliorate risk. The methods presented are not directly comparable to the AS3959 method for calculating RHF exposure (Standards Australia, 2009). Rather than the simple set-back distance (cleared space between vegetation and house) and peak RHF, this model uses a spatially continuous map of vegetation distribution to generate a detailed range (and therefore time) based RHF exposure potential profile for each house.

Without the availability of lidar data that underpinned Case Study One, the model presented makes the best use of limited the spatial detail provided by national vegetation datasets (ALUM and NCAS data at 25 m spatial resolution). It also shows that it is still possible to extend conventional AS3959 site-based assessments to incorporate the distribution of multiple vegetation fuel types surrounding the house, detailed topography and attenuation of radiant heat flux. The results show that there are links between the total accumulated energy at a house, the duration of exposure to greater than 12 $kW/m^2$ and the occurrence of house damage during the 2005 Wangary fire ($p(\chi^2) < 0.01$). This is despite relatively low levels of radiant heat generated by the grass fuel dominated fire.

Although this report provides an assessment of worst case spatial information, we do not suggest that the data used in this study is ideal for modelling potential RHF exposure. Detailed vegetation fuel structural information, such as that available from airborne lidar, would provide significantly more information on the vertical structure of vegetation and its variability over the landscape. Consequently, these data would provide significantly more confidence in modelling of RHF any relationships to house damage.

We consider that the levels of radiant heat estimated by the model were unlikely to have been the key mechanism for ignition during the Wangary fire. Strong relationships between modelled RHF and house damage are likely to have been due to correlations between radiant heat exposure, ember density and the probability of direct flame contact. The use of radiant heat as a surrogate for overall exposure is also the basis for AS3959 assessment. Given the relationships between modelled RHF and house damage shown in this report, we support the continued use of RHF as a primary means of assessing exposure. However, it is important to separate out the risks to houses from radiant heat and other ignition mechanisms because the appropriate response to each hazard, in terms of building design and fuel management, is different. Future work to explicitly model ember hazard and flame contact will add greater certainty to the assessment of overall hazard and provide a basis for more targeted actions to mitigate risk.

# 8 References


Baxter, J.T. and Russell, L.D. (1994). *Land Use Mapping Requirements for Natural Resource Management in the Murray–Darling Basin*. Project M305: Task 6. Department of Conservation and Natural Resources, Victoria.

Blanchi, R. and Leonard, J. (2008). Property safety: judging structural safety. In: J. Handmer and K. Haynes (eds.). *Community Bushfire Safety*. pp. 77–85.

Burrough, P. and McDonnell, R. (1998). *Principles of geographical information systems*. Oxford University Press.

Byram, G.M. (1959). Combustian of Fuels. In: K. P. Davis (ed.). *Forest Fire Control and Use*. McGraw-Hill, pp. 61–89.

CFA (2013). *Planning for Bushfire Victoria: Guidelines for meeting Victoria's bushfire planning requriements*.

Cheney, N., Gould, J. and McCaw, L. (1998). Project Vesta: research initiative into the effects of fuel structure and fuel load on behaviour of wildfires in dry eucalypt forest. Proceedings of the *13th Fire and Meteorology Conference*.

Cohen, J. (2004). Relating flame radiation to home ignition using modeling and experimental crown fires. *Canadian Journal of Forest Research*.

Drysdale, D. (1985). An Introduction to Fire Dynamics. Chichester, John Wiley and Sons.

Furby, S. (2002). *Land Cover Change : Specification for Remote Sensing Analysis, National Carbon Accounting System Technical Report*.

Gallant, J.C., Dowling, T.I., Read, A.M., Wilson, N., Tickle, P. and Inskeep, C. (2011). *1 second SRTM Derived Digital Elevation Models User Guide. Geoscience Australia*. Available from: www.ga.gov.au/topographic-mapping/digital-elevation-data.html.

Gould, J. (2005). *Development of Bushfire Spread of the Wangary Fire 10 and 11 th January 2005 Lower Eyre Peninsula South Australia*. Preliminary Report to South Australia State Coroner ' s Office and South Australia Country Fire Service.

Jupp, D.L.B., Culvenor, D.S., Lovell, J.L., Newnham, G.J., Strahler, a H. and Woodcock, C.E. (2009). Estimating forest LAI profiles and structural parameters using a ground-based laser called 'Echidna. *Tree physiology*. 29 (2). p.pp. 171–181.

Leonard, J. (2009). *Report to the 2009 Victorian Bushfires Royal Commission. Building performance in bushfires*. http://www.royalcommission.vic.gov.au/Documents/Document-files/Exhibits/TEN-066-001-0001.pdf.

Leonard, J. and Blanchi, R. (2006). *A study of the interaction between bushfire and community in the South Australian Wangary fire 2005*.

Leonard, J., Blanchi, R., Newnham, G., Culvenor, D., Siggins, A. and Opie, K. (2011). *Characterisation of interface fuels–literature review, Bushfire CRC report*.

McArthur, A.G. (1973a). *Forest Fire Danger Meter Mark V*. Forestry Research Institute, Forestry and Timber.

McArthur, A.G. (1973b). *Grassland Fire Danger Meter Mk IV*. Bush Fire Council of N.S.W. Officer Training Module CL/4 - Fire Behaviour Second Edition.

Nelson, R.M. (1980). *Flame Characteristics for Fires in Southern Fuels*. [Online]. Available from: USDA Forest Service Research Paper .

Noble, I.R., Bary, G.A.V. and Gill, A.M. (1980). McArthers fire danger meters expressed as equations. *Australian Journal of Ecology*. 5. p.pp. 201–203.

Siggins, A., Leonard, J., Newnham, G., Blanchi, R., Lipkin, F., Opie, K. and Culvenor, D. (2013). *Modelling Radiant Heat Exposure at the Urban Fringe - Pine Ridge Road, Kinglake West, Case Study*. CSIRO Report EP13821,.

Smith, B. (2005). *Report of Independent Review of Circumstances Surrounding Eyre Peninsula Bushfire of 10th and 11th January 2005 (Wangary Bushfire)*.

Standards Australia (2009). *Australian Standard ® Construction of buildings in bushfire-prone areas*.

Sullivan, A.L., Ellis, P.F. and Knight, I.K. (2003). A review of radiant heat flux models used in bushfire applications. *International Journal of Wildland Fire*.

Takeda, T., Oguma, H., Sano, T., Yone, Y. and Fujinuma, Y. (2008). Estimating the plant area density of a Japanese larch (Larix kaempferi Sarg.) plantation using a ground-based laser scanner. *Agricultural and Forest Meteorology*. 148 (3). p.pp. 428–438.

Teague, B., McLeod, R. and Pascoe, S. (2009). Victorian bushfires royal commission interim report. *Parliament of Victoria, Melbourne*.

Tippins, D., Nairn, J. and Watson, A. (2005). *Meteorological Aspects of the Black Tuesday Fires - Lower Eyre Peninsula, Tuesday 11 January 2005*.

Tran, H.C., Cohen, J.D. and Chase, R.A. (1992). Modeling ignition of structures in wildland/urban interface fires. In: *Proc 1st international fire and materials conference, Arlington, VA*. 1992, pp. 253–262.

Zárate, L., Arnaldos, J. and Casal, J. (2008). Establishing safety distances for wildland fires. *Fire Safety Journal*. 43 (8). pp. 565–575.